JOURNAL OF GEOPHYSICAL RESEARCH, VOL. 101, NO. A5, PAGES 10,673–10,680, MAY 1, 1996

Discrete, stimulated auroral kilometric radiation observed in the Galileo and DE 1 wideband data

J. D. Menietti

Department of Physics and Astronomy, University of Iowa, Iowa City

H. K. Wong

Aurora Sciences Inc., San Antonio, Texas

W. S. Kurth, D. A. Gurnett, L. J. Granroth, and J. B. Groene

Department of Physics and Astronomy, University of Iowa, Iowa City

Abstract. The Galileo spacecraft observed intense auroral kilometric radiation during the second Earth encounter in 1992. High-resolution frequency-versus-time spectrograms obtained by the wideband receiver of the plasma wave instrument on board the spacecraft often show discrete, negative-slope features each extending over a period of several seconds. These features may be due to impulsive wave generation and intrinsic velocity dispersion and/or a source stimulation by plasma waves traveling up the magnetic field line through the source region. We present several examples of these signatures, seen also on the Dynamics Explorer 1 satellite, and examine scenarios for their generation.

Introduction

Gurnett et al. [1979] and *Gurnett and Anderson* [1981] using ISEE data, *Benson et al.* [1988] using DE 1 data, and *Morioka et al.* [1981] with Exos B data have all reported examples of auroral kilometric radiation (AKR) fine structure in both the ordinary and extraordinary modes, indicating that AKR is emitted in discrete bursts lasting only a few seconds or less. Observed frequency drift rates of features are in the range 100 Hz/s $< R <$ tens of kilohertz per second. The bandwidth can be quite small ($<$ 1 kHz). *Gurnett et al.* [1979] suggest that the drifting features may be due to rising and falling source regions. The fine structures include not only drifting features but also discrete bands of near-monochromatic emission and other discrete features that are seen at the highest resolution available. Auroral roar is a relatively narrowband emission occurring near twice the electron gyrofrequency and first detected by *Kellogg and Monson* [1979]. Most recently, *LaBelle et al.* [1995] have reported similar structures in auroral roar emissions at frequencies of a few megahertz (2 or 3 times the local gyrofrequency). There are a number of theories that attempt to explain the source of the AKR fine structure observed. Such knowledge is necessary if we are to fully understand the details of the AKR generation mechanism. *Wu and Lee* [1979] have no doubt identified the general instability mechanism responsible for the emission, but as pointed out some years ago by *Melrose* [1986], the cyclotron maser mechanism would be an incomplete theory if it could not explain the timescales of wave growth associated with AKR fine structure.

Calvert [1982] has proposed that AKR fine structure can be explained by a feedback model, which requires radiation oscillations (similar to an optical laser) in a density enhancement region of diameter ≤25 km that converges with altitude. The source would emit radiation at its normal modes and would thus naturally explain monochromatic fine structure bands. Fine structure features that are observed to drift in frequency are explained in the feedback model by density gradients at the boundaries of the density enhancement region. *Melrose* [1986] has proposed a feedback model that depends on a phase-bunching mechanism and the wave trapping saturation model of VLF emission growth put forth by *Helliwell* [1967]. Melrose's theory of AKR fine structure depends critically on the assumption that the wave-particle interaction region for AKR growth has a parallel velocity intermediate between those of the particles and the waves. Occasional monochromatic signatures including bands of emission have been observed in the AKR fine structure. *Grabbe* [1982] presents examples of the latter features that he explains in terms of a three-wave generation mechanism based on ion cyclotron waves [*Grabbe et al.*, 1980]. *Farrell* [1995] has recently suggested that some monochromatic features in the AKR fine structure can be explained by free-energy electrons interacting with an oscillating density cavity boundary that has quasi-monochromatic wavelike motion. Adiabatic changes in the structure of the cavity can lead to drifting radio tones similar to those observed.

McKean and Winglee [1991] have performed one-dimensional particle-in-cell (P-I-C) simulations of AKR fine structure from sources associated with strong magnetic field gradients due to currents thought to be near or along the source field line. These authors find that rapidly drifting features ($>$10 kHz/s) are proportional to the growth rate (for positive drift rate) or nearly constant (for negative drift rate). For slowly drifting features (close to observed drifts) the rates are approximately proportional to the B-field gradient.

Understanding the source of AKR fine structure is critical to understanding details of the generation mechanism. The band-

Paper number 96JA00362.
0148-0227/96/96JA-00362$09.00

width of the fine structure, for instance, puts severe constraints on spatial growth rates as produced by the cyclotron maser instability. In this paper we will present observations of discrete negative-drifting "stripes" that, to our knowledge, have not been previously cited in the literature. These stripes are unique in appearance and therefore may have a unique source mechanism relative to the remainder of the auroral kilometric radiation. We will suggest two possible scenarios for the generation of such features.

Observations

As seen in Figure 1, Galileo approached the Earth from the evening sector where it observed intense AKR. The observations we report were made when Galileo was approximately 10 to 12 R_E distant from Earth during the second flyby. In Figure 2, we present a frequency-time spectrogram of the plasma wave data obtained by the low-, medium-, and high-frequency receivers of the plasma wave system on board Galileo. The wave intensity is gray coded with the most intense emissions appearing as black. The data were taken on December 8, 1992, prior to closest approach (CA). The intense AKR is seen in Figure 2 to extend in frequency from about 50 to over 600 kHz in the time interval from 1030 to about 1430 UT.

In Figure 3 we display a frequency-time spectrogram of the wideband data for a 1-min time period beginning at 1307:04. The frequency range of the plot is from 40 to 80 kHz. Seen in Figure 3 are somewhat diffuse features that have both positive and negative frequency drifts. These features are similar to those discussed in the past by *Gurnett et al.* [1979] and *Benson et al.* [1988]. In addition, indicated on the plot is a narrow (in time) feature with negative slope extending from about 65 kHz down to about 40 kHz. This feature almost has the appearance of a stripe or arc, but because of low intensity and diffusion of the signal, it is not clear if there is any curvature at the lowest frequencies. This signature is one of the best examples of the discrete stripes we have observed, because it extends in frequency for perhaps 30 kHz, longer than many others. These signatures are not unique and appear at other times in the Galileo wideband data as shown in Figure 4 for a time period about 20 min later than in Figure 3. The features are observed near the end of the time interval with about the same slope and frequency extent as those stripes observed in Figure 3. The features are not unique to the Galileo data. In Figure 5 we display wideband data obtained from the plasma wave instrument on board the DE 1 spacecraft as it approached a source region of intense AKR in the midaltitude, evening-sector auroral region. Similar features are observed near the end of the spectrogram in the frequency range from about 100 kHz down to about 65 kHz. Again, the slope is about the same, within a factor of 2. The stripes have been observed at numerous times in the Galileo Earth Encounter 2 wideband data, all with about the same characteristics. Only a few samples of the voluminous DE 1 wideband data set have been examined, and the stripes were seen in some of the auroral passes. No clear examples of stripes with positive slope were observed in the Galileo or DE data, but a comprehensive

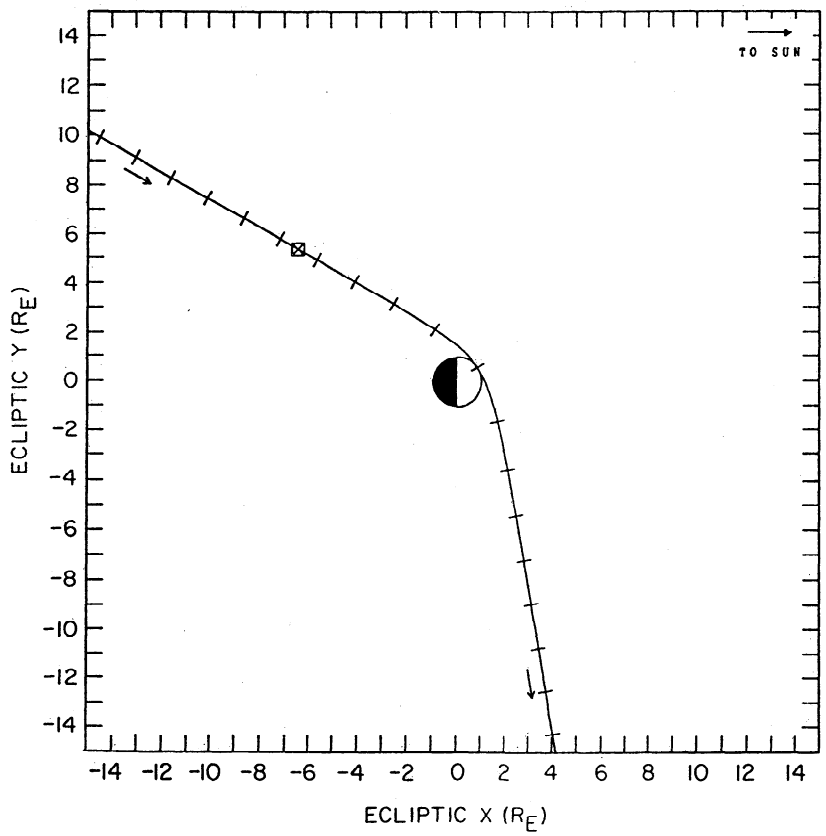

Figure 1. Galileo trajectory centered on closest approach to Earth at about 1510 UT on December 8, 1992. The plot is in the Earth-based ecliptic *x-y* plane, and the tick marks are 20 min apart. The nightside auroral region auroral kilometric radiation (AKR) sources were clearly visible to Galileo (position at 1310 UT is indicated by the square).

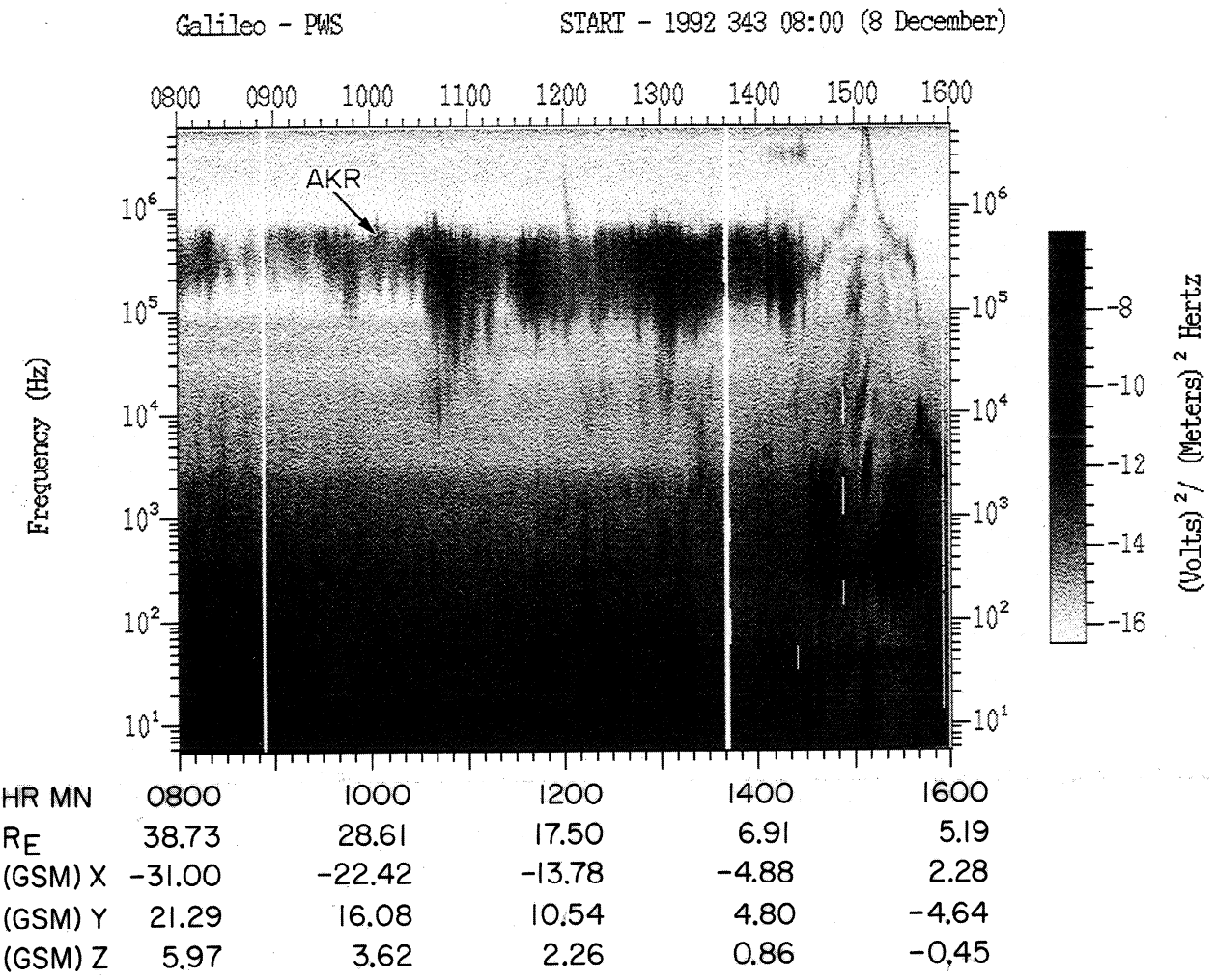

Figure 2. Frequency-versus-time spectrogram with the wave intensity gray coded. The frequency range extends from 1 Hz to 5.6 MHz on a log scale and includes emissions from the low-, medium-, and high-frequency swept frequency receivers. The intense AKR is seen as the black emission centered at about 200 kHz in the time range from 0800 to about 1430 UT. The closest approach (CA) is identified by the peak in the narrowbanded upper hybrid frequency near the maximum frequency of the plot at approximately 1510 UT.

investigation of the data remains to be conducted. To summarize, the stripes are very discrete in frequency, with a downward and approximately linear drift on a frequency-time spectrogram.

Analysis

Because of its isolated nature and relatively large frequency extent, we have chosen the signature indicated in Figure 3 for detailed study. We have carefully measured the data points of this signature and attempted to fit them to generalized curves. The best fit appears to be to a linear function with a slope of about -9 kHz/s, as shown in Figure 6. In Figure 6 the point near 50 kHz departs most from the fitting line, but in our analysis we assume that *df/dt* is a constant. While some of the other stripes may have a small curvature at the lowest frequencies, because of the faintness of the signals and diffusion it is not certain.

Two possible generation mechanisms for such signatures were analyzed. First, we consider the possible impulsive stimulation of the entire AKR source region along a field line as indicated in the cartoon in Figure 7. In this scenario, the signature could be produced by an intrinsic dispersion due to the source mechanism. For gyroemission, the wave group velocity decreases as the wave frequency approaches the local gyrofrequency, Ω_{ce}, and this group velocity decreases as the gyrofrequency decreases. Thus we first consider the possibility of impulsively stimulated emission at frequencies very near Ω_{ce} at different points along the field line. We envision AKR generated with maximum growth rate at a frequency close to Ω_{ce} such that $V_g/c \ll 1$.

To quantitatively investigate this possibility, we consider a ring-beam electron distribution as follows:

$$f = \delta(v_\perp - v_{\perp 0})\ \delta(v_z - v_{z0})/(2\pi v_\perp) \quad (1)$$

After *Winglee* [1985] we can write the warm plasma dispersion relation for AKR as

$$k^2 c^2/\omega^2 = \epsilon_{xx} + \epsilon_{xy}^2/\epsilon_{xx} \quad (2)$$

where ϵ is the dielectric tensor as defined in the appendix of *Winglee* [1985]. For this analysis a number of assumptions are made in order to simplify the calculations:

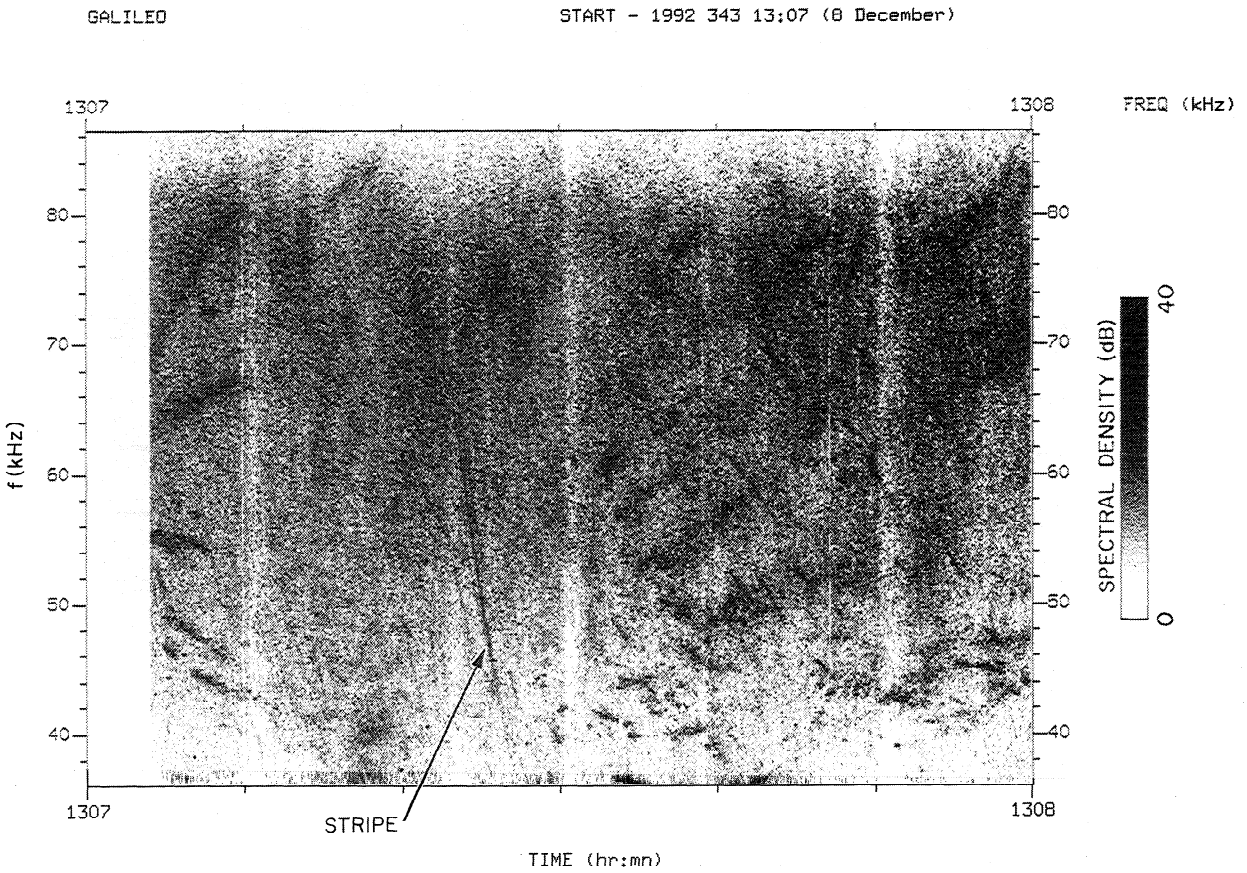

Figure 3. The wideband AKR data are plotted in frequency-time spectrogram with the intensity gray coded using a relative scale. Frequency range is from 40 to 80 kHz on a linear scale. The plot starts at 1307:04 and extends for 1 min. The fine structure is visible as dark positive- and negative-slope features. Note the discrete negative-slope feature indicated by the arrow.

$$k_z^2 \ll k_\perp^2$$
$$\omega^2 \gg k_z^2 c^2$$
$$k_\perp^2 v_\perp^2/\Omega_{ce}^2 \ll 1 \qquad (3)$$
$$v^2/c^2 \ll 1$$

where k is the wave vector, ω is the angular frequency, ω_{pc} is the electron plasma frequency of the cold component, and ω_{pE} is the plasma frequency of the energetic component. The dispersion relation is given by equations (A1) and (B1) through (B9) of the appendix of *Winglee* [1985]. The group velocity can be written as a function of a number of parameters

$$V_g = f(\omega_{pc}, \omega_{pE}, \Omega_{ce}, v_\parallel, v_\perp, v_b) \qquad (4)$$

where $v_\parallel$ and $v_\perp$ are the parallel and perpendicular velocities of the ambient electrons and v_b is the beam velocity. In Figure 8, we show a plot of V_g versus f for the specific case of f_{ce} = 60 kHz, f_{pc} = 3.8 kHz, f_{pE} = 1.2 kHz, $v_\parallel/c$ = 0.1, $v_\perp/c$ = 0.07, and $(k_\parallel v_b)/\Omega_{ce}$ = 0.01. These parameters may be reasonable for a source located in the auroral region at an altitude of about 1 R_E. As can be seen, V_g drops off rapidly as ω approaches Ω_{ce}. In order to generate a simulated dispersion, it is necessary to calculate V_g for different frequencies along the magnetic field line within the AKR source region. Thus it is necessary to know the ratio ω/Ω_{ce} at each source point. However, as *Wong et al.* [1982] have pointed out for a more realistic loss cone distribution (compare their Figure 5 and Figure 6), the maximum growth rate of AKR depends on ω/Ω_{ce} and on the ratio of energetic to background electrons. For a value of ω/Ω_{ce} = 1.015 and ω_p = 4.0 kHz at all points within the source region, we obtain the dispersion curve shown in Figure 9, which is directly compared with the data. While the data show a linear frequency dependence, the calculated dispersion is not linear. In addition, the calculated dispersion curve would require that the source region (where the plasma parameters would be applicable) be unphysically large (~10 R_E in diameter). It is also particularly disturbing that the AKR maximum growth rate and thus the result obtained in Figure 9 are rather strongly dependent on the ratio of energetic to background electron number density, n_E/n_b, and on ω/Ω_{ce}. For all of these reasons we do not believe that intrinsic dispersion is the mechanism responsible for the observed signatures in the AKR fine structure spectrum.

Wave Stimulation

An alternative source of the observed wave signature is stimulation of AKR by a wave that propagates up the field line through the source region, as depicted in the cartoon of Figure 10. The bandwidth of the assumed gyroemission observed in Figure 2 requires that the source region extend about 3000 km along the field line. The observed signature (typical of most) lasts about 3.5 s, so the stimulating wave must have a group

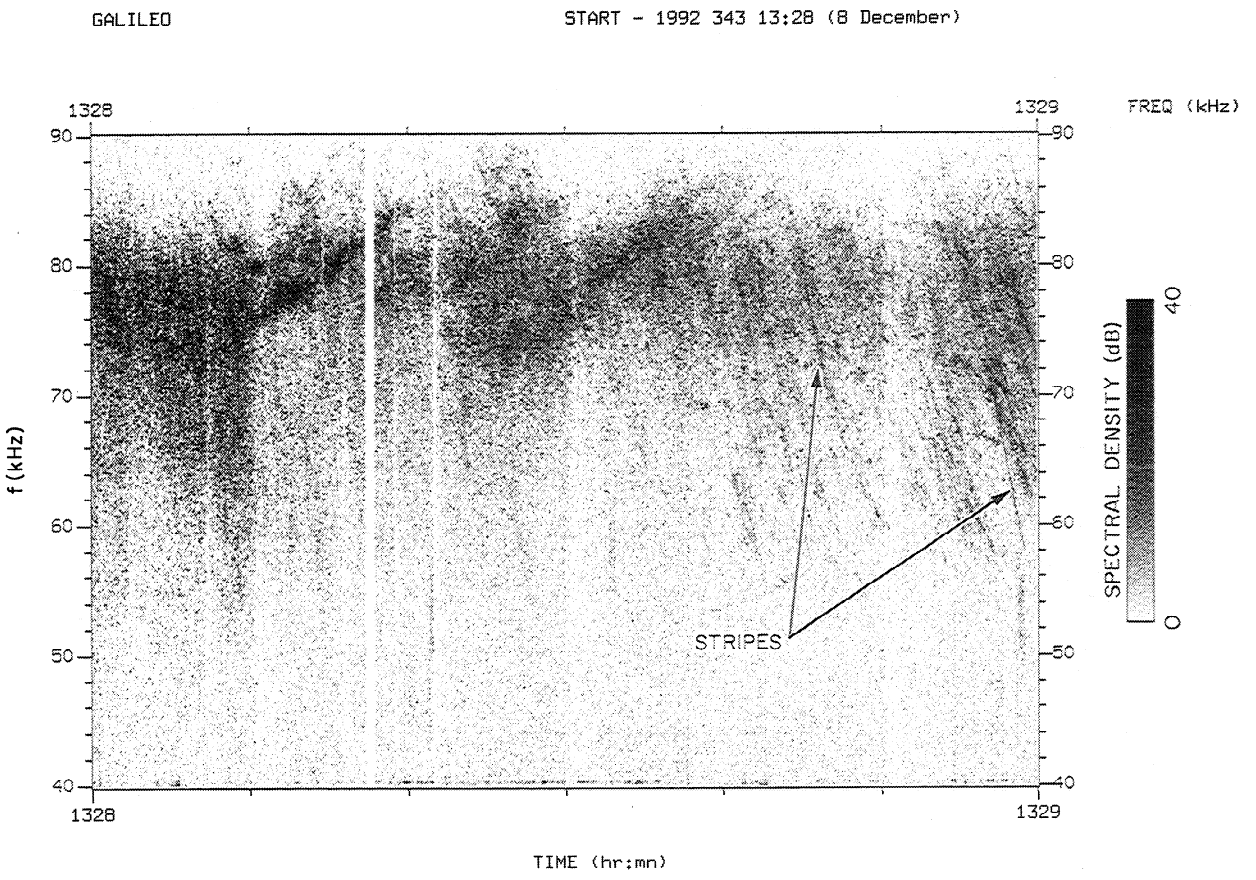

Figure 4. A wideband frequency-versus-time spectrogram of AKR for a period of time about 20 min later than the observations shown in Figure 3. The frequency range is linear from 40 to 90 kHz, and the time extent of the plot is 1 min. The discrete, negative-slope features (similar to Figure 3) are seen more clearly toward the end of the plot.

velocity along the field line of about 1000 km/s. There are a number of candidates for such waves that have been observed regularly at frequencies near and below both the hydrogen and oxygen ion cyclotron frequencies [cf. *Gurnett et al.*, 1984]. These emissions include whistler mode, Alfven waves, and electromagnetic ion cyclotron (EMIC) waves. In the cold plasma approximation, we consider each of these waves for appropriate parameters in the AKR source region.

Candidate Waves of Stimulation

For whistler mode waves, the dispersion relation is

$$\mu^2 = 1 + \omega_p^2/[\omega(\Omega_{ce} \cos \Psi - \omega)]$$
$$\mu' = d(\mu\omega)/d\omega$$
$$V_g = c/\mu'$$

where Ψ is the wave normal angle. For the parameters $f \sim 2$ kHz, $f_c \sim 65$ kHz, and 4 kHz $> f_p >$ 100 kHz, we obtain $V_g > 0.1c$.

For Alfven waves, the dispersion relation is

$$V_g = c/\sqrt{1+(4\pi\rho/B^2)}$$

where ρ is the plasma mass density and B is the magnetic field intensity. For the parameters $B > .02$ gauss and $\rho > 6.7 \times 10^{-21}$ kg/m^3, we obtain $V_g/c > 3.3 \times 10^{-2}$.

For electromagnetic ion cyclotron (EMIC) waves, the dispersion relation ($N^2 \gg 1$) is

$$V_g = \frac{2cN(\Omega_{ci} - \omega)\omega}{\omega_{pi}^2\left[\frac{\Omega_{ci}}{(\Omega_{ci} - \omega)} - \frac{\omega_{pe}^2}{\omega_{pi}^2}\frac{(\Omega_{ci} - \omega)}{\Omega_{ce}}\right]}$$

where

$$N^2 = \left[\frac{\omega_{pi}^2}{(\Omega_{ci} - \omega)} - \frac{\omega_{pe}^2}{\Omega_{ce}}\right]\Big/\omega$$

For the parameters $f_c(O^+) = 1.36$ Hz, $f_p(O^+) = 11.7$ Hz, $f = 1.27$ Hz, $f_{ce} = 40$ kHz, and $f_{pe} = 4$ kHz, we obtain $V_g \sim 905$ km/s (O^+), while for $f_c(H^+) = 21.7$ Hz, $f_p(H^+) = 93.5$ Hz, $f = 20.9$ Hz, $f_{ce} = 40$ kHz, and $f_{pe} = 4$ kHz, we obtain $V_g \sim 908$ km/s (H^+).

Using kinetic theory, *Lin et al.* [1989] have investigated beam-driven EMIC waves for a specific case in the dayside cusp region. Taking the measured parameters for their observed case, $f = 62$ Hz, $f_p(H+) = 413$ Hz, $f_c(H+) = 65$ Hz, $n_{beam}/n_b = 0.1$, $V_b/c = 4.67 \times 10^{-4}$, $f_{pe} = 17.7$ kHz, and $f_{ce} = 150$ kHz, we obtain $V_g \sim 900$ km/s.

It is clear that EMIC waves have field-aligned group velocities of the correct magnitude to be candidates for AKR stimulation in the source region, while the other wave modes considered do not.

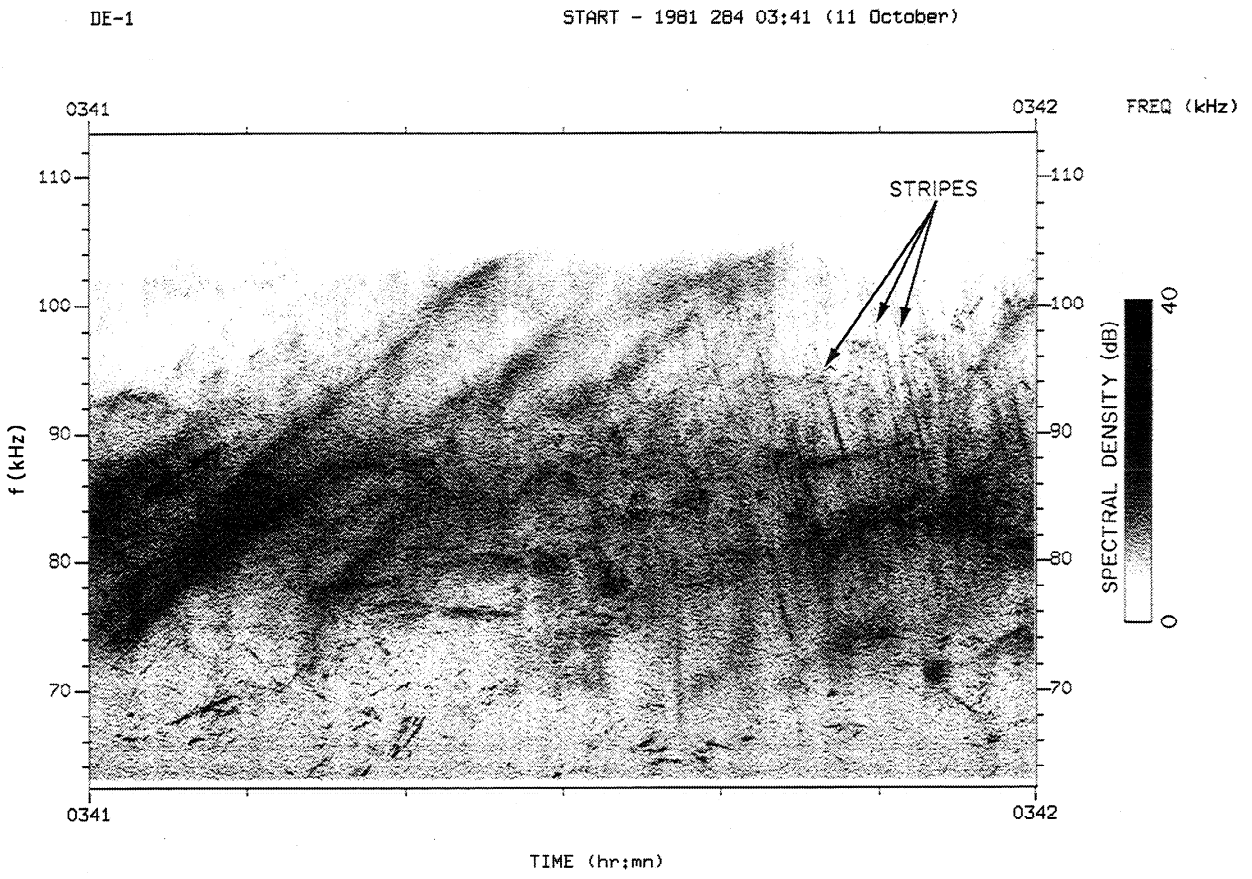

Figure 5. Wideband data obtained by the plasma wave instrument on board DE 1 as it approached the AKR source region in the midaltitude nightside auroral region. The frequency scale is in kilohertz and the time extent is 1 min. Again, the intensity scale is relative. Seen on the plot are large positive-slope frequency drifting features but also the discrete, negative-slope features (similar to Figures 3 and 4) more clearly visible in the last half of the plot.

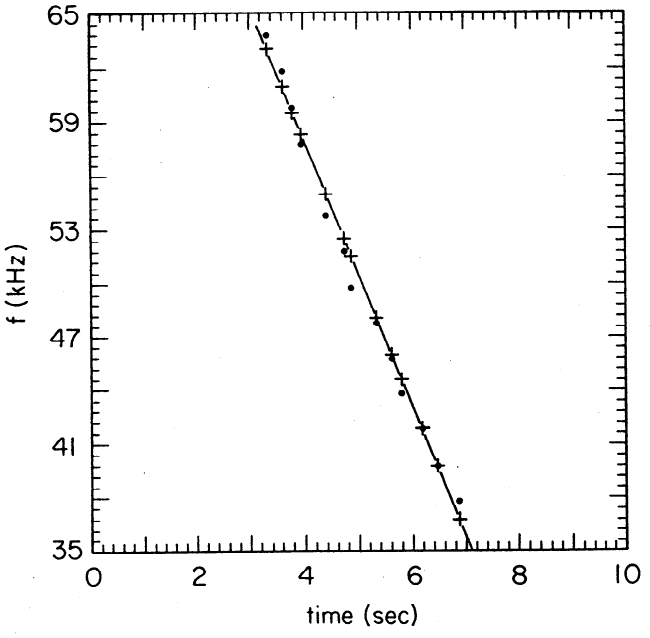

Figure 6. Data measured from the spectrogram and fitted to a generalized function. The best fit is to a linear curve with negative slope of about -9 kHz/s. The data points are shown as solid circles.

Summary and Discussion

Discrete "stripelike" structures in the AKR wideband data are observed not infrequently in both Galileo Earth flyby data and in the DE 1 auroral zone data. A statistical study of the data remains to be conducted, however. These signatures are characterized by the following features: frequency extent ~30 kHz, $\Delta t \leq 4$ s, $f \propto 1/t$. We have considered two possible sources for the signatures: (1) impulsive stimulation of the entire source region with intrinsic dispersion at all frequencies within the AKR source region and (2) stimulation of AKR within the source region by a wave traveling up the magnetic field line. AKR triggering has been suggested previously by *Calvert* [1981, 1985] and most recently by *Calvert* [1995]. In the latter studies, AKR was observed associated with type II and III radio bursts, but the AKR was not observed to be dispersive as in the observations here reported.

We have assumed a ring-beam distribution of particles in order to investigate impulsive stimulation of AKR. However, not only does the resulting dispersion not match the observations, which show a linear dependence on inverse time, but also, for reasonable plasma parameters, the group velocities are much larger than those required to reproduce the observed signatures.

Stimulation of the source region by electromagnetic plasma waves traveling away from Earth through the AKR source region has also been investigated. A wave traveling up the magnetic

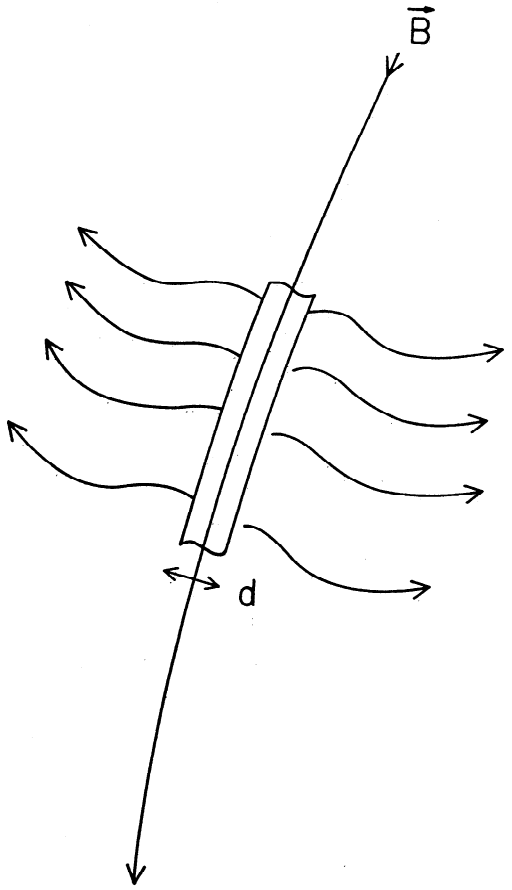

Figure 7. This cartoon depicts a possible source of the discrete features. AKR is seen emanating impulsively from the entire source region that extends along the field line. In this scenario, the gyroemission at higher frequencies at lower altitude would have a higher group velocity than the lower frequencies at higher altitude.

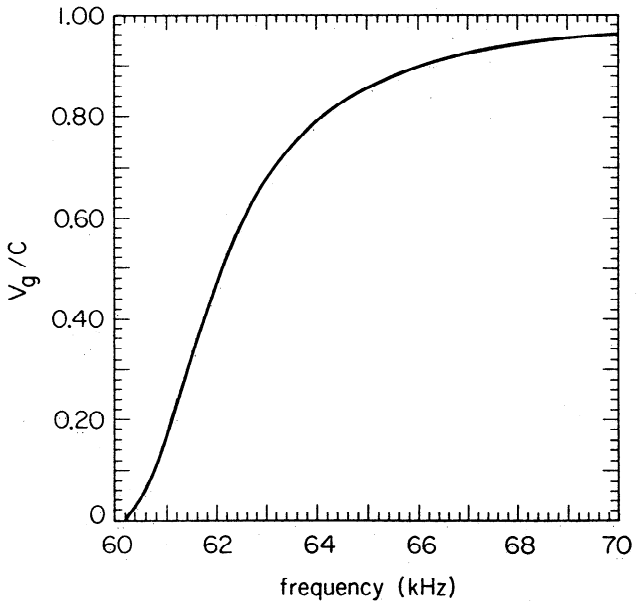

Figure 8. The group velocity is plotted versus frequency for AKR emission near Ω_{ce} = 60 kHz resulting from a ring-beam electron distribution. Other plasma parameters are listed in the text. The group velocity rapidly decreases to zero near the gyrofrequency as expected.

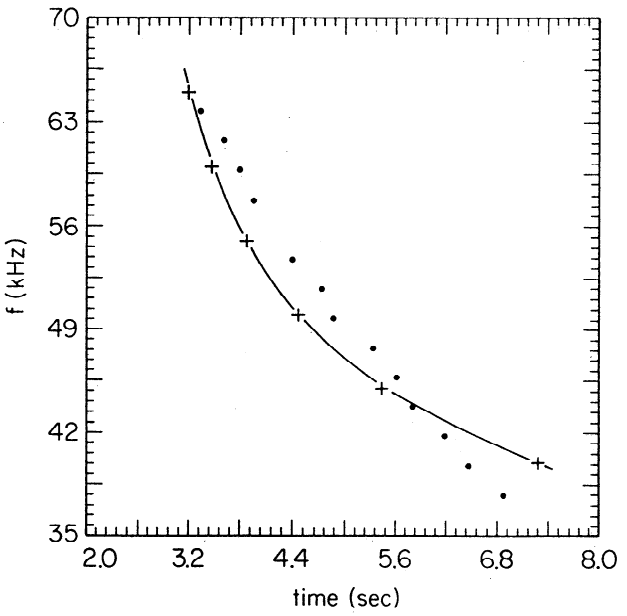

Figure 9. Superimposed on the data is the calculated intrinsic dispersion curve for very specific plasma parameters in the source region. The calculated values show a curve, while the data points are nearly linear.

field line with a group velocity of about 1000 km/s would pass through the AKR source region (40 kHz $< f <$ 65 kHz) in about 3.5 s. Whistler mode and Alfven waves would have group velocities that are too large in the AKR source region, but electromagnetic ion cyclotron waves cannot be ruled out. The association of EMIC waves with auroral field lines (the source region of AKR) is well established. *Gurnett et al.* [1984] reported Dynamics Explorer observations on auroral field lines of strong electromagnetic emissions at frequencies less than the hydrogen and oxygen cyclotron frequencies. *Temerin et al.* [1986, 1993] have proposed that EMIC waves are the source of flickering aurora, a result recently supported by sounding rocket observations of *Lund et al.* [1995]. *Erlandson et al.* [1994] have presented Freja observations of EMIC waves associated with inverted-V electron precipitation on auroral field lines. The proposed scenario of EMIC stimulation of certain AKR spectral signatures is thus not inconsistent with these other auroral observations.

Gurnett et al. [1984] and *Lund et al.* [1995] both reported that low-frequency auroral region observations indicate that most of the Poynting flux is downward. The stimulated emission suggested in our work requires waves traveling up the field line in order to explain the observed negative frequency drift. However, *Temerin and Lysak* [1984] have postulated that upward propagating EMIC waves below the heaviest ion gyrofrequency could become resonant with ions and result in transverse ion acceleration. The observations of *Erlandson et al.* [1994] were consistent with this scenario. *Temerin et al.* [1986, 1993] have modeled flickering aurora showing the correlation of electron data with standing EMIC waves. These waves have sources near the bottom of or just below the acceleration region at frequencies near or below the ion cyclotron frequency and propagate downward to reflect near the ion-hybrid frequency. Such observations would be consistent with our model of upward propagating EMIC waves that penetrate the acceleration region after reflection, for example. In this scenario it would be

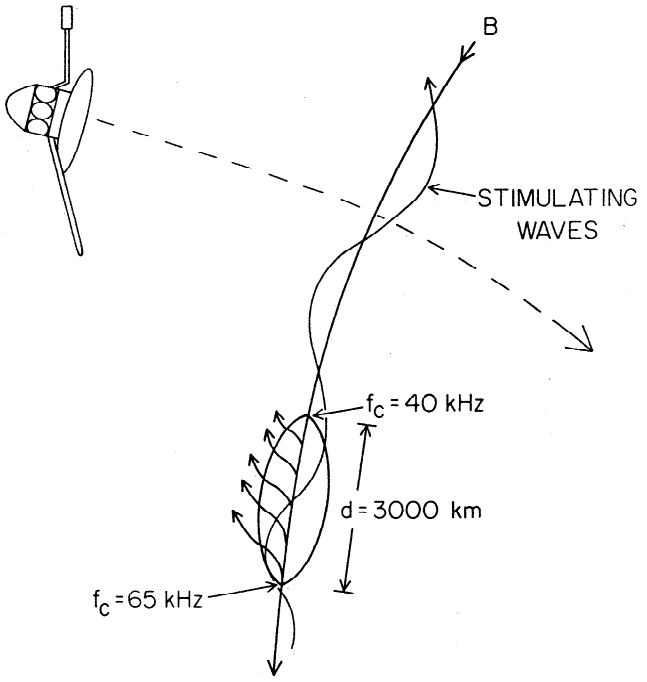

Figure 10. An AKR source region being stimulated by a field-aligned wave traveling up the magnetic field line. For a total distance, *d*, of about 3000 km, the wave group velocity would have to be about 950 km/s to produce a discrete feature that persists for about 3.5 s as observed.

necessary for the bottom of the acceleration region to extend below the altitude of the ion cyclotron frequency. We would also add that since both the Galileo and DE wideband data sets used in this study have not been systematically studied, we cannot rule out the possibility that observations of stripes with positive slope may yet be observed.

The actual mechanism by which the AKR emission is stimulated has not been critically investigated, but we suggest that as the stimulating wave propagates through the AKR source region, it modifies the ratio ω_p / Ω_{ce} and/or the plasma distribution in pitch angle or energy. Finally, we emphasize that our work has been confined to explain only the discrete stripelike features such as those indicated in Figures 3-5. We do not suggest that all of the discrete fine structure signatures are generated by plasma wave stimulation. At this point it is not clear what role, if any, wave stimulation by other wave modes has in the generation of AKR.

Acknowledgments. We were aided by comments made by M. Temerin on the topic of EMIC waves. We would like to thank K. Kurth and JooHee Chung for typesetting the manuscript. This work was funded by contract 958779 with the Jet Propulsion Laboratory.

The Editor thanks M. Trimpi and R. E. Erlandson for their assistance in evaluating this paper.

References

Benson, R. F., M. M. Mellott, R. L. Huff, and D. A. Gurnett, Ordinary mode auroral kilometric radiation fine structure observed by DE 1, *J. Geophys. Res.*, *93*, 7515, 1988.

Calvert, W., The stimulation of auroral kilometric radiation by type III solar radio bursts, *Geophys. Res. Lett.*, *8*, 1091, 1981.

Calvert, W., A feedback model for the source of auroral kilometric radiation, *J. Geophys. Res.*, *87*, 8199, 1982.

Calvert, W., Auroral kilometric radiation triggered by type II solar radio bursts, *Geophys. Res. Lett.*, *12*, 377, 1985.

Calvert, W., An explanation for auroral structure and the triggering of auroral kilometric radiation, *J. Geophys. Res.*, *100*, 14,887, 1995.

Erlandson, R. E., L. J. Zanetti, M H. Acuña, A. I. Eriksson, L. Eliasson, M. H. Boehm, and L. G. Blomberg, Freja observations of electromagnetic ion cyclotron ELF waves and transverse oxygen ion acceleration on auroral field lines, *Geophys. Res. Lett.*, *21*, 1855, 1994.

Farrell, W. M., Fine structure of auroral kilometric radiation: A Fermi acceleration process?, *Radio Sci.*, *30*, 961, 1995.

Grabbe, C. L., Theory of fine structure of auroral kilometric radiation, *Geophys. Res. Lett.*, *9*, 155, 1982.

Grabbe, C., K. Papadopoulos, and P. Palmadesso, A coherent nonlinear theory of auroral kilometric radiation, I, Steady state model, *J. Geophys. Res.*, *85*, 3337, 1980.

Gurnett, D. A., and R. R. Anderson, The kilometric radio emission spectrum: Relationship to auroral acceleration processes, in *Physics of Auroral Arc Formation, Geophys. Monogr. Ser.*, *Vol. 25*, edited by S.-I. Akasofu and J. R. Kan, p. 341, AGU, Washington, D.C., 1981.

Gurnett, D. A., R. R. Anderson, F. L. Scarf, R. W. Fredericks, and E. J. Smith, Initial results from the ISEE 1 and 2 plasma wave investigation, *Space Sci. Rev.*, *23*, 103, 1979.

Gurnett, D. A., R. L. Huff, J. D. Menietti, J. L. Burch, J. D. Winningham, and S. D. Shawhan, Correlated low-frequency electric and magnetic noise along the auroral field lines, *J. Geophys. Res.*, *89*, 8971, 1984.

Helliwell, R. A., A theory of discrete VLF emissions from the magnetosphere, *J. Geophys. Res.*, *72*, 4773, 1967.

Kellogg, P. J., and S. J. Monson, Radio emissions from the aurora, *Geophys. Res. Lett.*, *6*, 297, 1979.

LaBelle, J., M. L. Trimpi, R. Brittain, and A. T. Weatherwax, Fine structure of auroral roar emissions, *J. Geophys. Res.*, *100*, 21,953, 1995.

Lin, C. S., H. K. Wong, J. Koga, and J. L. Burch, Excitation of low-frequency waves by auroral electron beams, *J. Geophys. Res.*, *94*, 1327, 1989.

Lund, E. J., et al., Observation of electromagnetic oxygen cyclotron waves in a flickering aurora, *Geophys. Res. Lett.*, *22*, 2465, 1995.

McKean, M. E., and R. M. Winglee, A model for the frequency fine structure of auroral kilometric radiation, *J. Geophys. Res.*, *96*, 21,055, 1991.

Melrose, D. B., A phase-bunching mechanism for fine structures in auroral kilometric radiation and Jovian decametric radiation, *J. Geophys. Res.*, *91*, 7970, 1986.

Morioka, A., H. Oya, and S. Miyatake, Terrestrial kilometric radiation observed by satellite JIKKIKEN (EXOS-B), *J. Geomagn. Geoelectr.*, *33*, 37, 1981.

Temerin, M., and R. L. Lysak, Electromagnetic ion cyclotron mode (ELF) waves generated by auroral electron precipitation, *J. Geophys. Res.*, *89*, 2489, 1984.

Temerin, M., J. McFadden, M. Boehm, C. W. Carlson, and W. Lotko, Production of flickering aurora and field-aligned electron flux by electromagnetic ion cyclotron waves, *J. Geophys. Res.*, *91*, 5769, 1986.

Temerin, M., C. Carlson, and J. P. McFadden, The acceleration of electrons by electromagnetic ion cyclotron waves, in *Auroral Plasma Dynamics, Geophys. Monogr. Ser.*, *Vol. 80*, edited by R. L. Lysak, p. 155, AGU, Washington, D.C., 1993.

Winglee, R. M., Fundamental and harmonic electron cyclotron maser emission, *J. Geophys. Res.*, *90*, 9663, 1985.

Wong, H. K., C. S. Wu, F. J. Ke, R. S. Schneider, and L. F. Ziebell, Electromagnetic cyclotron-loss-cone instability associated with weakly relativistic electrons, *J. Plasma Phys.*, *28*, 503, 1982.

Wu, C. S., and L. C. Lee, A theory of the terrestrial kilometric radiation, *Astrophys. J.*, *230*, 621, 1979.

L. J. Granroth, J. B. Groene, D. A. Gurnett, W. S. Kurth, and J. D. Menietti, Department of Physics and Astronomy, University of Iowa, Iowa City, IA 52242. (e-mail: ljg@space.physics.uiowa.edu, jbg@space.physics.uiowa.edu, donald-gurnett@uiowa.edu, william-kurth@uiowa.edu, jdm@space.physics.uiowa.edu)

H. K. Wong, Aurora Sciences Inc., Suite 215, 4502 Centerview Drive, San Antonio, TX 78228.

(Received November 17, 1995; revised January 24, 1996; accepted January 26, 1996.)